Zitierweise: *Angew. Chem. Int. Ed.* **2021**, *60*, 7564–7569
Internationale Ausgabe: doi.org/10.1002/anie.202015170
Deutsche Ausgabe: doi.org/10.1002/ange.202015170

Chromophores

Melanin-Inspired Chromophoric Microparticles Composed of Polymeric Peptide Pigments

Ayala Lampel, Scott A. McPhee, Salma Kassem, Deborah Sementa, Tlalit Massarano, James M. Aramini, Ye He, and Rein V. Ulijn**

Abstract: *Melanin and related polyphenolic pigments are versatile functional polymers that serve diverse aesthetic and protective roles across the living world. These polymeric pigments continue to inspire the development of adhesive, photonic, electronic and radiation-protective materials and coatings. The properties of these structures are dictated by covalent and non-covalent interactions in ways that, despite progress, are not fully understood. It remains a major challenge to direct oxidative polymerization of their precursors (amino acids, (poly-)phenols, thiols) toward specific structures. By taking advantage of supramolecular pre-organization of tyrosine-tripeptides and reactive sequestering of selected amino acids during enzymatic oxidation, we demonstrate the spontaneous formation of distinct new chromophores with optical properties that are far beyond the range of those found in biological melanins, in terms of color, UV absorbance and fluorescent emission.*

Nature provides a tremendous source of inspiration for the development of sustainable polymeric materials with precisely defined structural and optical properties. Examples include high-performance materials based on mussel-inspired adhesives,[1,2] adaptive pigmentary,[3] and pigment-based coloration.[4–6] Melanin pigments are now recognized as promising materials with potential uses in various applications,[7] due to their optical,[8] electronic[9–12] and radiation-protection[13] properties. The biosynthesis of animal melanins is a multistep oxidative polymerization process that is understood to rely on templated pre-organization and enzymatic oxidative-polymerization of specific amino acids.[7,14] The chemical nature of the amino acid substrates dictates the properties in these systems, with tyrosine giving rise to the brown-black pigment eumelanin, while a mixture of tyrosine and cysteine results in formation of the yellow-red polymeric pigment pheomelanin. Both types of melanin play a role in sun protection through broadband absorption in the ultra-violet (UV) and visible spectra and they are weakly fluorescent.[15]

Inspired by eumelanin/pheomelanin biosynthesis,[7] and taking advantage of supramolecular peptide self-assembly[16–19] to create tunable supramolecular templates, it was previously demonstrated that enzymatic oxidation of short peptides enables the formation of polymeric pigments with structures and properties that are dictated by the peptide sequence.[20–23] We set out to test if firstly amino acids (including cysteine) could be incorporated as observed in pheomelanin to change the optical properties through formation of new chromophores.

We first developed a method to produce melanin-like particles with a defined micro-structure as a reactive scaffold for subsequent oxidative incorporation of amino acids. (Figure 1 a,b). Based on the observation that lysines are featured in rapidly polymerizing mussel adhesives[1] and interact with aromatic residues through cation-π interactions,[2] we used the tripeptide Lys-Tyr-Phe (KYF)—which is known to form nanofibrous gels[24]—as a supramolecular precursor. At physiological pH in aqueous buffer, the peptide self-assembles into a translucent hydrogel composed of a physically entangled network of nanofibrils (Figure 1 c, Figure S1, Supporting Information).[24] We then used mushroom tyrosinase to oxidize the KYF gel [resulting in $(KYF)_{ox}$], upon which a red-brown color appears within minutes, which over 24 h matures into a suspension with a colloidal film forming at the oxygen-rich air/liquid interface (Figure 1 c, Figure S1a). Oxidation of the pre-assembled peptide is not expected to result in formation of 5,6-dihydroxyindole intermediates as the tyrosine amine is occupied in a peptide bond, but rather in formation of catechol and quinone side chains that can further polymerize (Figure 1 a). We note therefore that while the formation process of these polymeric peptide pigments is inspired by natural melanins, they are themselves not strictly melanins, hence we refer to them as melanin-like or melanin

[*] Dr. A. Lampel, S. A. McPhee, Dr. S. Kassem, Dr. D. Sementa, Dr. J. M. Aramini, Dr. Y. He, Prof. R. V. Ulijn
Advanced Science Research Center (ASRC) at the Graduate Center, City University of New York (CUNY)
85 St Nicholas Terrace, New York, NY 10031 (USA)
E-mail: rulijn@gc.cuny.edu
Dr. A. Lampel, T. Massarano
The Shmunis School of Biomedicine and Cancer Research, George S. Wise Faculty of Life Sciences, Tel Aviv University
Tel Aviv 69978 (Israel)
E-mail: ayalalampel@tauex.tau.ac.il
Dr. A. Lampel
The Center for Nanoscience and Nanotechnology Tel Aviv University
Tel Aviv 69978 (Israel)
and
Sagol Center for Regenerative Biotechnology Tel Aviv University
Tel Aviv 69978 (Israel)
Prof. R. V. Ulijn
Department of Chemistry, Hunter College
City University of New York
695 Park Avenue, New York, NY 10065 (USA)
and
Ph.D. programs in Biochemistry and Chemistry
The Graduate Center of the City University of New York
New York, NY 10016 (USA)
Supporting information and the ORCID identification number(s) for the author(s) of this article can be found under: https://doi.org/10.1002/anie.202015170.

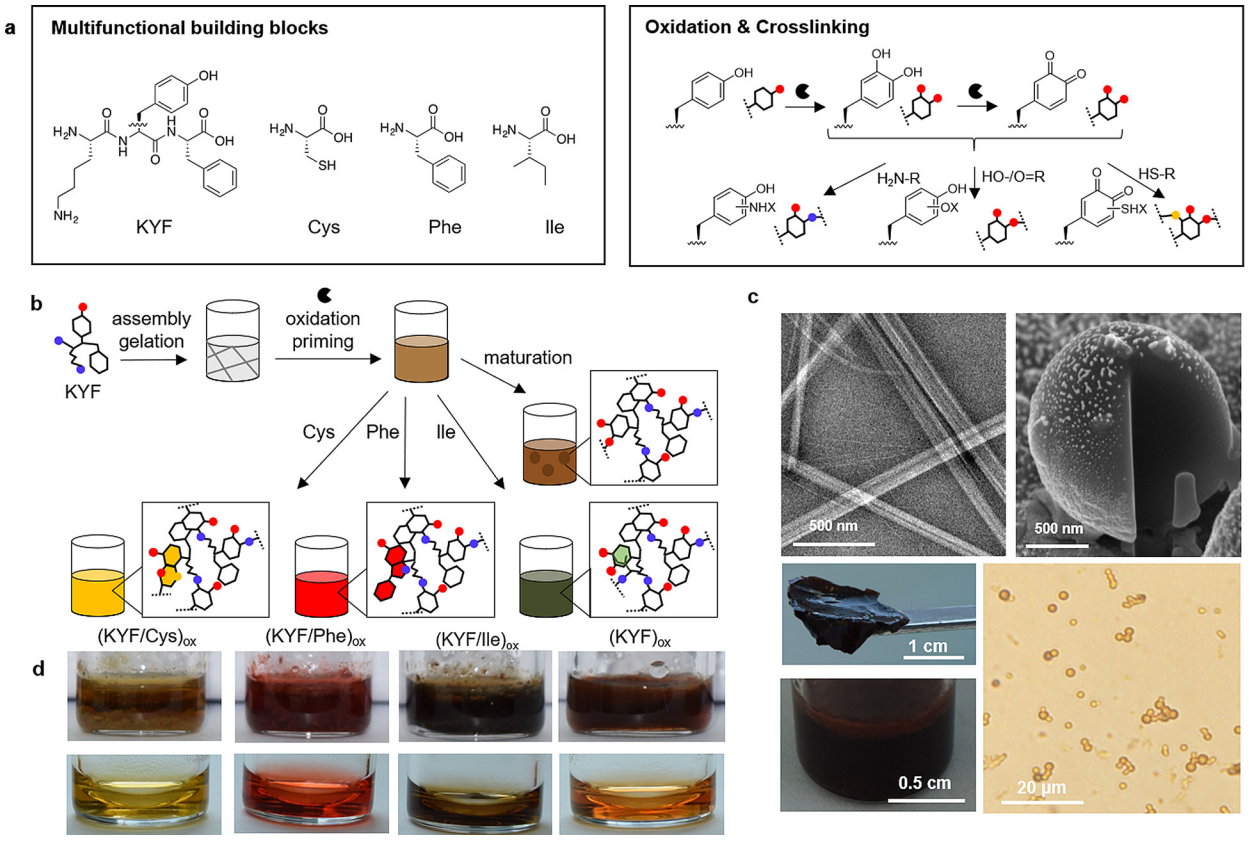

Figure 1. Spontaneous formation of new polymeric peptide chromophores. a) *Left panel*: chemical structures of multifunctional self-assembling peptide (KYF) and amino acid building blocks. *Right panel*: chemical structures and schematic representation of the tyrosine side chain following enzymatic oxidative-polymerization and addition of amino acids. Reactive groups are indicated: OH/O = red, NH_2 = blue, SH = yellow. b) KYF self-assembles into nanofibers that pre-organize tyrosine residues for enzymatic oxidative-polymerization. 3 hours of enzymatic oxidation is either followed by the addition of Cys, Phe, or Ile resulting in further oxidation and the emergence of new polymeric peptide chromophores, or continued without amino acid addition resulting in the formation of polymeric microparticles. c) *Top*: TEM image of KYF gel fibers (left) and SEM image (using FIB) of $(KYF)_{ox}$ microparticle (right). *Bottom*: macroscopic (left) and optical microscopy (right) images of (KYF)ox material and microparticles. d) Macroscopic images of reaction mixtures (top) and supernatants (bottom) following addition of amino acids and maturation clearly showing the emergence of colored species.

inspired. Transmission electron microscopy (TEM) time course analysis shows that spherical particles with a diameter of <10 nm start to form from the fibers immediately after tyrosinase addition. The particles' diameter increases over time up to ≈ 2 µm (Figure S1b). Optical and scanning electron microscopy (SEM and TEM) analyses confirmed the formation of microparticles following peptide oxidation (Figure 1c, Figure S1d). Size distribution dynamic light scattering (DLS) analysis after 24 h of oxidation shows three populations of particles with a diameter of ≈ 150 nm, 1 µm, and 5 µm (Figure S1c), where the last peak might represent accumulation of 1–3 particles as observed by optical microscopy and bright field confocal microscopy (Figure 1c, Figure S1d). Microscopy analysis of $(KYF)_{ox}$ microparticles resuspended in 50% methanol confirmed that they are polymeric structures rather than physical aggregates of $(KYF)_{ox}$ oligomers (Figure S1d,e). We note that the particles are stabilized by a combination of covalent and non-covalent interactions and the full characterization of the oligomeric composition is beyond the scope of the current paper.

To test whether new chromophores could be formed by the reaction of amino acids with the oxidized tyrosine, we first studied the addition of cysteine (Cys), as a known precursor for pheomelanin,[25–27] and then aromatic phenylalanine (Phe), basic histidine (His) and aliphatic alanine, valine, leucine, and isoleucine (Ala, Val, Leu, and Ile), which are, to our knowledge, not known precursors for biological melanins. Due to their variable hydrophobic side chain groups they might change the polarity of the particles and thus change their optical properties. Each amino acid was added to the $(KYF)_{ox}$ reaction mixture 3 hours after initiation in order to allow oxidative priming and oligomerization and to increase particles' abundance in the mixture, as observed by confocal microscopy. Cys addition after 3 hours resulted in an immediate color change of the reaction mixture from red-brown to yellow. By contrast, addition of His and Phe resulted in readily observable color change to red and intense red, respectively, and addition of either of the aliphatic amino acids (Ala, Val, Leu or Ile) resulted in a brown/green color (Figure S2). These results suggested the in situ formation of new chromophores (Figure 1d, Figure S2a). Next, we focused

on the chromophoric materials formed by addition of Cys, Phe and Ile, as these amino acids present distinctive side chain groups and the resulting materials showed the most profound coloration and unique UV/Vis absorbance.

After 24 hours of reaction, we performed optical analysis of both the isolated solid microparticles, as well as the remaining solution (supernatant) phase (Figure 1 d shows that comparable coloration is clearly observable in both phases). We investigated the fluorescent properties of the chromophoric materials in the reaction mixtures and supernatants (Figure 2 a,b). 2D excitation-emission spectroscopy of the $(KYF)_{ox}$ reaction mixture reveals a λ_{ex} of 449 nm and intense λ_{em} at 533 nm (Figure 2 a). The chromophores formed by the co-oxidation of KYF/Cys, Phe and Ile give rise to emission spectra that are clearly different from that of $(KYF)_{ox}$, both for the reaction mixture and supernatant. $(KYF/Cys)_{ox}$ has a broader and blue shifted excitation, which correlates with the yellow coloration while a 40 nm redshifted λ_{em} is observed for $(KYF/Phe)_{ox}$, and far-red fluorescence for $(KYF/Ile)_{ox}$ ($\lambda_{ex} = 600$ nm, $\lambda_{em} = 621$ nm). Notably for Phe, significant narrowing of the excitation band compared to $(KYF/Cys)_{ox}$ and an increase in emission intensity are observed (Figure 2 a). The fluorescence of the supernatants showed a similar trend (Figure 2 b). UV/Vis spectra of the supernatants of $(KYF)_{ox}$ and $(KYF/Cys)_{ox}$ show broadband UV/vis absorbance (Figure 2 d), similar to melanins.[15] In contrast, $(KYF/Phe)_{ox}$ has an additional distinctive and intense absorbance at 501 nm, which correlates with the red coloration, while $(KYF/Ile)_{ox}$ and all the other chromophoric materials formed by addition of aliphatic amino acids have an additional lower intensity absorbance at 620 nm, correlating to the observed brown/green color (Figure 2 d, Figure S2b).

Next, we studied the optical properties of microparticles using high-resolution confocal microscopy and show that they

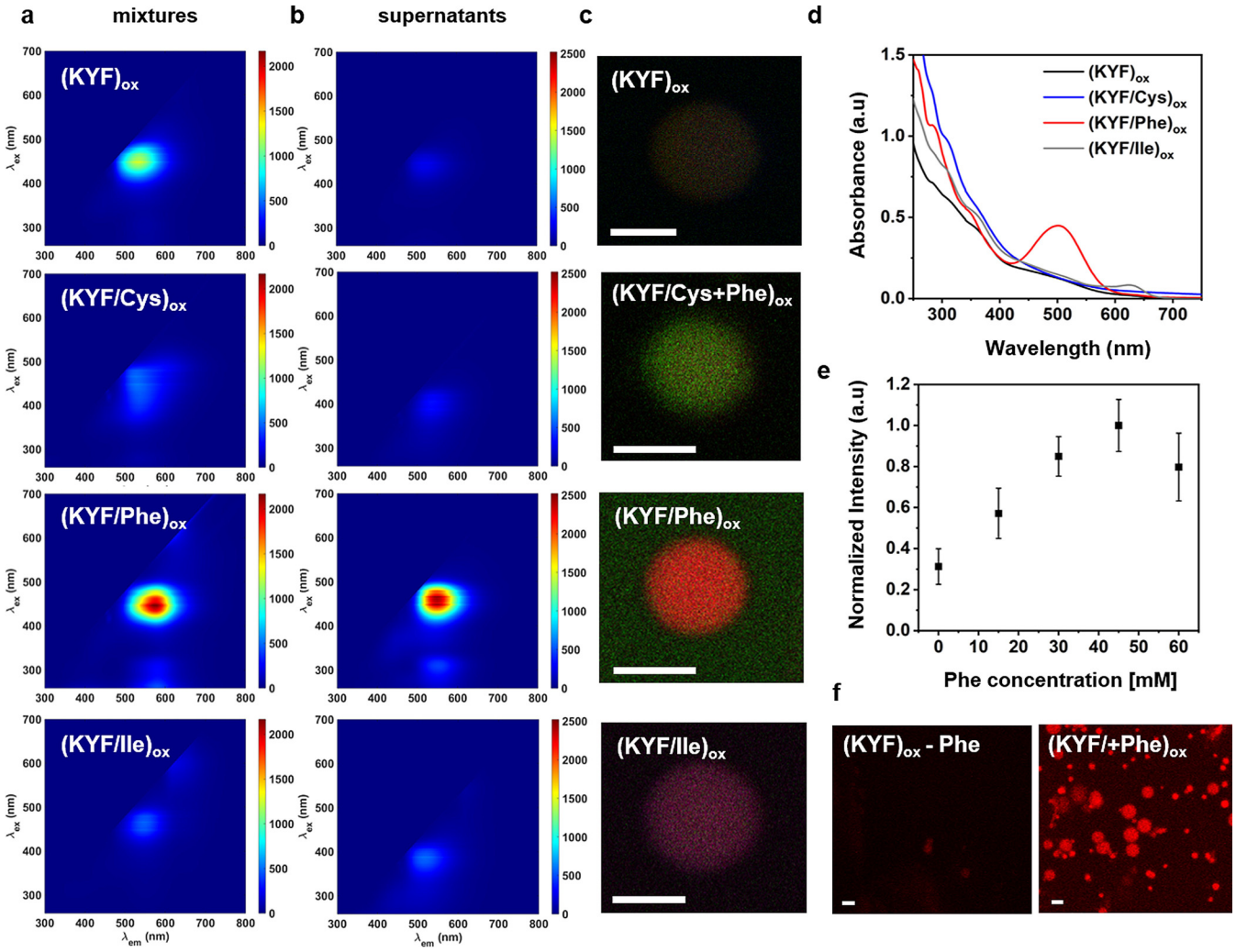

Figure 2. Optical analysis of polymeric peptide chromophoric materials. a,b) 2D excitation (*y*-axis)-emission (*x*-axis) spectra of the reaction mixtures (a) or supernatants (b) of $(KYF)_{ox}$, $(KYF/Cys)_{ox}$, $(KYF/Phe)_{ox}$, $(KYF/Ile)_{ox}$. Maximal intensity indicated in red. c) Confocal microcopy images of particles formed by addition of amino acids showing merged fluorescence at excitation wavelengths: 514, 561, and 633 nm. Scale bar = 2 µm. d) UV/Vis spectra of the polymeric peptide chromophores supernatants diluted 4-fold (e) Fluorescence intensity of microparticles following addition of increasing concentrations of Phe. Values represent average of 10 particles, error bars are indicated. f) Confocal microscopy images of microparticles formed with or without Phe addition. Excitation wavelength is 561 nm. Scale bar = 2 µm.

can be tuned across the green (Cys/Phe), yellow-red (Phe) and far-red (Ile) regions of the spectrum (Figure 2c). Note that, unlike Phe or Ile inclusion by the microparticles, addition of Cys results in a mixture of crystalline polyhedral structures (Figure S3,S4), which may be related to the high reactivity of the thiol which results in extensive polymerization and loss of spherical shape. Therefore, we sought to provide a competing precursor by supplying Cys in combination with Phe or Ile. We found that a 2-fold molar excess of Phe and Ile over Cys could be used with partial retention of particle morphology and in situ incorporation to form new chromophores in mixed morphology of polyhedral structures and microparticles (Figure S4) with green fluorescence observed for both (Figure 2c, Figures S5,S6). These results show that the side chain of the added amino acid dictates the fluorescence properties of the particles and that multiple amino acid precursors can be incorporated simultaneously.

We subsequently monitored the incorporation of increasing concentrations of Phe into individual microparticles to assess whether the level of incorporation could be regulated. A dose-dependent increase in the particles' emission intensity was observed following Phe addition (Figure 2e) while a static, and overall weak signal was observed in the absence of Phe (Figure 2f). These findings demonstrate that the microparticles reactively incorporate the Phe residues to form new chromophores in a quantitative manner and suggest that the particles may serve as cumulative sensors to quantify metabolites (exemplified by Phe) by irreversible incorporation and consequent signal generation.

A general model of eumelanin structures that is commonly suggested is a heterogeneous aggregate of stacked oligomers of 5,6-dihydroxyindole (DHI) and 5,6-dihydroxyindole-2-carboxylic-acid (DHICA),[28–30] which may include porphyrin-like tetramers.[31,32] Yet, the chemical structure of the oligomeric units and the nature of their interactions have not been fully determined, with evidence of the polymeric nature of polydopamine materials only reported recently.[33] We reasoned that analyzing the supernatant from reaction mixtures would help shed light on the chemical composition of the in situ produced chromophores. Liquid chromatography-mass spectrometry (LCMS) analysis of the $(KYF/Cys)_{ox}$ supernatant revealed the presence of species indicating that Cys is incorporated to the oxidized tripeptide via a similar mechanism to that proposed for pheomelanin synthesis[34] (Figures S7–S11). LCMS analysis of the Phe reaction supernatant showed that the absorbance maxima at around 500 nm primarily results from one set of closely related compounds. To elucidate the chemical structure, the most abundant peptide chromophore identified by LCMS of the $(KYF/Phe)_{ox}$ supernatant was purified using preparative HPLC (termed $(KYF/Phe)_{chrom}$) after 24 h of oxidation, and eluted as two major peaks with an identical mass. The chromophore was freeze-dried and re-dissolved for the NMR and spectroscopy analyses. ^{13}C and ^{15}N labelled $(KYF/Phe)_{chrom}$ were synthesized and purified following the same procedure. LCMS and NMR studies were used to determine the structure of $(KYF/Phe)_{chrom}$ (Figure 3a–c, Figures S7–S27, NMR data Figures S29–S41). The NMR studies clearly show the loss of

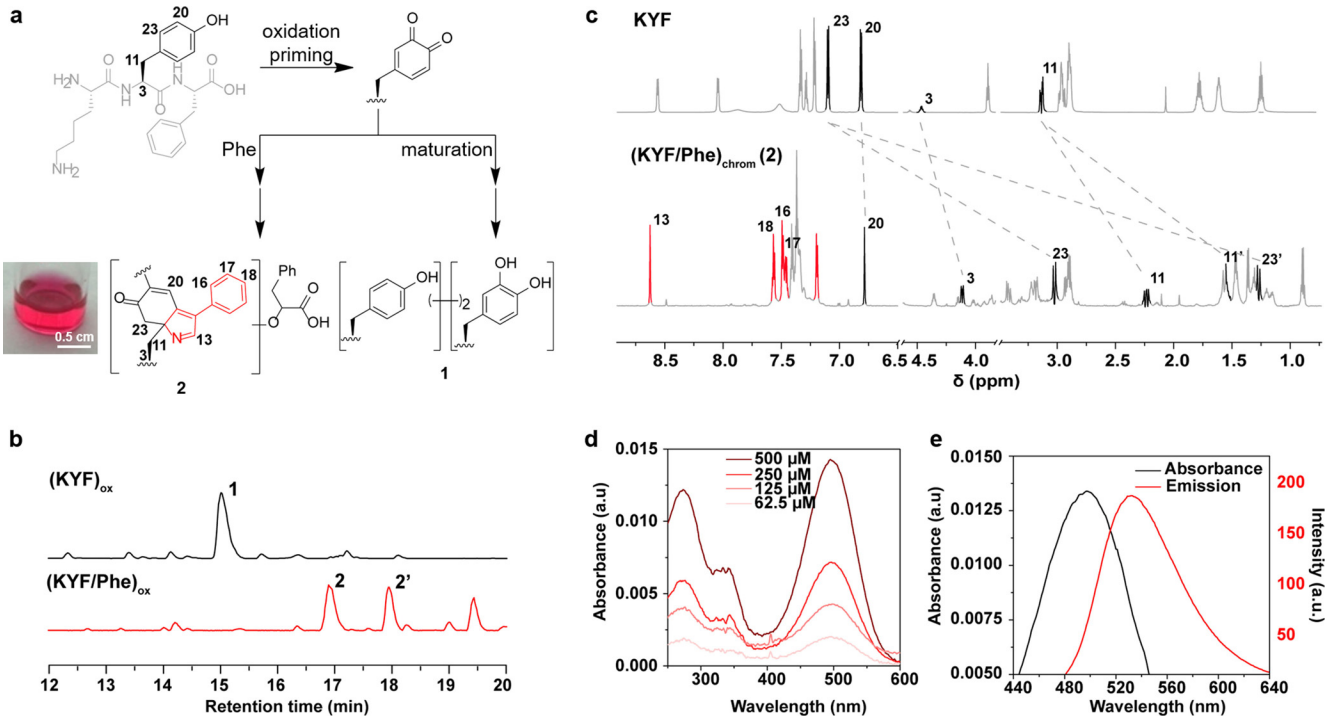

Figure 3. Characterization of peptide chromophores. a) Structures of major compounds identified following the chemical transformation of KYF upon oxidation, maturation and inclusion of Phe. A macroscopic image of $(KYF/Phe)_{chrom}$ solution is presented. b) Partial LCMS traces of reaction supernatants with assignment of identified major species. c) Partial ^{1}H NMR spectra (800 MHz, 298 K, 5% D2O in 10 mM Tris buffer) of KYF (top) and $(KYF/Phe)_{chrom}$ (bottom). Dashed lines connect resonances indicative of the chemical transformation of the tyrosine ring and the emergence of the new chromophore. For full proton assignments see Supplementary Information NMR section. d) UV/Vis absorbance spectra of $(KYF/Phe)_{chrom}$ at varying concentrations. e) Absorbance and emission spectra of $(KYF/Phe)_{chrom}$ showing $\lambda_{abs} = 500$ nm and $\lambda_{emission} = 530$ nm.

aromaticity in the tyrosine ring and the presence of a newly formed pyrrole ring fused to the 6-membered ring (Figures 3a, c). The isotope labelling studies indicate that the pyrrole ring comes from the incorporated Phe. This would presumably happen through the reaction of Phe amine and oxidized KYF quinone intermediate via a Strecker degradation-type sequence of events. The chemical formula determined by MS suggests that two residues of Phe have been incorporated, and this was also seen by NMR. One residue is incorporated as the fused 3-phenylpyrrole ring, while the other residue seems to have undergone a deamination process (supported by MS analysis of ^{15}N labelled Phe reaction, Figure S20). NMR analysis suggests it has been incorporated as a phenylpropionic acid (Figure S29). However, it shows no correlation either with the KYF backbone, the side chains or newly formed ring system. This has led us to conclude the suggestive structure shown in Figure 3a. By contrast, The chromophore responsible for the 620 nm absorbance in $(KYF/Ile)_{ox}$ was not sufficiently abundant to be detected by LC-DAD of the supernatant and enable structural characterization.

Next, we analyzed the absorbance and fluorescence of the purified $(KYF/Phe)_{chrom}$. The chromophore has three λ_{max} at 275 nm, 335 nm, and 499 nm, with λ_{ex} of 464 nm and λ_{em} of 533 nm (Figure 3d,e). The absorbance λ_{max} of $(KYF/Phe)_{chrom}$ was found to be similar to that of the $(KYF/Phe)_{ox}$ supernatant although its λ_{em} is blue-shifted compared to that of the supernatant and reaction mixture. In contrast, the fluorescence of natural melanin was found to be aggregation dependent.[35] The relative quantum yield of $(KYF/Phe)_{chrom}$, obtained using a pyrromethene 546 standard (see Methods), was found to be 2–4%. This value is slightly higher than that of known water-soluble chromophores that are used for staining biological samples including Congo red ($\phi = 1.1\%$)[36] and much higher than the reported quantum yield of biological melanins ($\phi = 0.3\%$).[37–41]

We show that a combination of pre-organization through self-assembly and controlled oxidative incorporation of amino acids with variable side chain functionality can give rise to polymeric chromophores which can be directed to specified optical properties by simply varying their nature and incorporate them into the mixture. Reactions of multifunctional building blocks typically give rise to poorly controlled mixtures, yet this work demonstrates that convergence to specific new chromophores is achievable through selection of building blocks, compartmentalization, and supramolecular preorganization. The directed reactive incorporation of functionality in complex reaction mixtures provides a new paradigm for materials synthesis that may shed light on the emergence of chemical chromophores from simple building blocks in early living systems.[42] More specifically, this approach holds promise for the scalable synthesis of melanin materials with photonic properties that are tightly controlled, and go beyond those available in natural melanins, for applications in surface coatings, photoacoustic imaging and biophotonics,[43] biosensing,[5] and cosmetics.

Acknowledgements

This research was supported by the U.S. Air Force Office of Scientific Research (grant FA9550-19-1-0111). We thank M. Y. Sfeir (Photonics Initiative at the Advanced Science Research Center, The Graduate Center CUNY) for help with quantum yield measurements, S. Zhang for the help with SEM imaging, M. Palha and D. Karson for help with UV/Vis measurements.

Conflict of interest

The authors declare no conflict of interest.

Keywords: bioinspired materials · melanin · peptide self-assembly · pigments · supramolecular materials

[1] H. Lee, S. M. Dellatore, W. M. Miller, P. B. Messersmith, *Science* **2007**, *318*, 426–430.
[2] M. A. Gebbie, W. Wei, A. M. Schrader, T. R. Cristiani, H. A. Dobbs, M. Idso, B. F. Chmelka, J. H. Waite, J. N. Israelachvili, *Nat. Chem.* **2017**, *9*, 473–479.
[3] T. L. Williams, S. L. Senft, J. Yeo, F. J. Martín-Martínez, A. M. Kuzirian, C. A. Martin, C. W. DiBona, C.-T. Chen, S. R. Dinneen, H. T. Nguyen, C. M. Gomes, J. J. C. Rosenthal, M. D. MacManes, F. Chu, M. J. Buehler, R. T. Hanlon, L. F. Deravi, *Nat. Commun.* **2019**, *10*, 1–15.
[4] M. Xiao, Z. Hu, Z. Wang, Y. Li, A. D. Tormo, N. Le Thomas, B. Wang, N. C. Gianneschi, M. D. Shawkey, A. Dhinojwala, *Sci. Adv.* **2017**, *3*, e1701151.
[5] C. Shillingford, C. W. Russell, I. B. Burgess, J. Aizenberg, *ACS Appl. Mater. Interfaces* **2016**, *8*, 4314–4317.
[6] A. L. Davis, K. N. Thomas, F. E. Goetz, B. H. Robison, S. Johnsen, K. J. Osborn, *Curr. Biol.* **2020**, *30*, 3470–3476.
[7] M. d'Ischia, K. Wakamatsu, F. Cicoira, E. Di Mauro, J. C. Garcia-Borron, S. Commo, I. Galván, G. Ghanem, K. Kenzo, P. Meredith, A. Pezzella, C. Santato, T. Sarna, J. D. Simon, L. Zecca, F. A. Zucca, A. Napolitano, S. Ito, *Pigm. Cell Melanoma Res.* **2015**, *28*, 520–544.
[8] F. G. Kapp, J. R. Perlin, E. J. Hagedorn, J. M. Gansner, D. E. Schwarz, L. A. O'Connell, N. S. Johnson, C. Amemiya, D. E. Fisher, U. Wölfle, E. Trompouki, C. M. Niemeyer, W. Driever, L. I. Zon, *Nature* **2018**, *558*, 445–448.
[9] Y. J. Kim, W. Wu, S.-E. Chun, J. F. Whitacre, C. J. Bettinger, *Proc. Natl. Acad. Sci. USA* **2013**, *110*, 20912–20917.
[10] M. Sheliakina, A. B. Mostert, P. Meredith, *Mater. Horiz.* **2018**, *5*, 256–263.
[11] E. Valois, R. Mirshafian, J. H. Waite, *Sci. Adv.* **2020**, *6*, eaaz6486.
[12] A. B. Mostert, S. B. Rienecker, C. Noble, G. R. Hanson, P. Meredith, *Sci. Adv.* **2018**, *4*, eaaq1293.
[13] E. Dadachova, R. A. Bryan, X. Huang, T. Moadel, A. D. Schweitzer, P. Aisen, J. D. Nosanchuk, A. Casadevall, *PLoS One* **2007**, *2*, e457.
[14] D. M. Fowler, A. V. Koulov, C. Alory-Jost, M. S. Marks, W. E. Balch, J. W. Kelly, *PLoS Biol.* **2005**, *4*, e6.
[15] P. Meredith, B. J. Powell, J. Riesz, S. P. Nighswander-Rempel, M. R. Pederson, E. G. Moore, *Soft Matter* **2006**, *2*, 37–44.
[16] S. Zhang, *Nat. Biotechnol.* **2003**, *21*, 1171–1178.
[17] T. Aida, E. W. Meijer, S. I. Stupp, *Science* **2012**, *335*, 813–817.
[18] M. J. Webber, E. A. Appel, E. W. Meijer, R. Langer, *Nat. Mater.* **2016**, *15*, 13–26.
[19] A. Levin, T. A. Hakala, L. Schnaider, G. J. L. Bernardes, E. Gazit, T. P. J. Knowles, *Nat. Rev. Chem.* **2020**, *4*, 615–634.

[20] M. Vij, R. Grover, V. Gotherwal, N. A. Wani, P. Joshi, H. Gautam, K. Sharma, S. Chandna, R. S. Gokhale, R. Rai, M. Ganguli, V. T. Natarajan, *Biomacromolecules* **2016**, *17*, 2912 – 2919.
[21] B. Sun, A. D. Ariawan, H. Warren, S. C. Goodchild, M. in het Panhuis, L. M. Ittner, A. D. Martin, *J. Mater. Chem. B* **2020**, *8*, 3104 – 3112.
[22] A. Lampel, S. A. McPhee, H. A. Park, G. G. Scott, S. Humagain, D. R. Hekstra, B. Yoo, P. Frederix, T. D. Li, R. R. Abzalimov, S. G. Greenbaum, T. Tuttle, C. Hu, C. J. Bettinger, R. V. Ulijn, *Science* **2017**, *356*, 1064 – 1068.
[23] S. M. M. Reddy, E. Raßlenberg, S. Sloan-Dennison, T. Hesketh, O. Silberbush, T. Tuttle, E. Smith, D. Graham, K. Faulds, R. V. Ulijn, N. Ashkenasy, A. Lampel, *Adv. Mater.* **2020**, *32*, 2003511.
[24] P. W. Frederix, G. G. Scott, Y. M. Abul-Haija, D. Kalafatovic, C. G. Pappas, N. Javid, N. T. Hunt, R. V. Ulijn, T. Tuttle, *Nat. Chem.* **2015**, *7*, 30 – 37.
[25] A. D. Schweitzer, R. C. Howell, Z. Jiang, R. A. Bryan, G. Gerfen, C.-C. Chen, D. Mah, S. Cahill, A. Casadevall, E. Dadachova, *PLoS One* **2009**, *4*, e7229.
[26] A. Napolitano, M. De Lucia, L. Panzella, M. d'Ischia, *Photochem. Photobiol.* **2008**, *84*, 593 – 599.
[27] S. Ito, *Pigm. Cell Res.* **1989**, *2*, 53 – 56.
[28] M. d'Ischia, A. Napolitano, V. Ball, C. T. Chen, M. J. Buehler, *Acc. Chem. Res.* **2014**, *47*, 3541 – 3550.
[29] G. W. Zajac, J. M. Gallas, J. Cheng, M. Eisner, S. C. Moss, A. E. Alvarado-Swaisgood, *Biochim. Biophys. Acta Gen. Subj.* **1994**, *1199*, 271 – 278.
[30] W. Li, Z. Wang, M. Xiao, T. Miyoshi, X. Yang, Z. Hu, C. Liu, S. S. C. Chuang, M. D. Shawkey, N. C. Gianneschi, A. Dhinojwala, *Biomacromolecules* **2019**, *20*, 4593 – 4601.
[31] C.-T. Chen, V. Ball, J. J. de Almeida Gracio, M. K. Singh, V. Toniazzo, D. Ruch, M. J. Buehler, *ACS Nano* **2013**, *7*, 1524 – 1532.
[32] Y. J. Kim, A. Khetan, W. Wu, S.-E. Chun, V. Viswanathan, J. F. Whitacre, C. J. Bettinger, *Adv. Mater.* **2016**, *28*, 3173 – 3180.
[33] P. Delparastan, K. G. Malollari, H. Lee, P. B. Messersmith, *Angew. Chem. Int. Ed.* **2019**, *58*, 1077 – 1082; *Angew. Chem.* **2019**, *131*, 1089 – 1094.
[34] S. Ito, *Pigment Cell Res.* **2003**, *16*, 230 – 236.
[35] J. B. Nofsinger, J. D. Simon, *Photochem. Photobiol.* **2001**, *74*, 31 – 37.
[36] M. O. Iwunze, *Spectrosc. Lett.* **2010**, *43*, 16 – 21.
[37] J. B. Nofsinger, T. Ye, J. D. Simon, *J. Phys. Chem. B* **2001**, *105*, 2864 – 2866.
[38] M. Xiao, M. D. Shawkey, A. Dhinojwala, *Adv. Opt. Mater.* **2020**, *8*, 2000932.
[39] S. Zhang, M. Xiao, Y. Zhang, Y. Li, H. Liu, G. Han, B. Rathi, K. Lyu, L. Wu, *Anal. Chim. Acta* **2020**, 1105, 208 – 213.
[40] Y. Zou, X. Chen, P. Yang, G. Liang, Y. Yang, Z. Gu, Y. Li, *Sci. Adv.* **2020**, *6*, eabb4696.
[41] P. Yang, S. Zhang, X. Chen, X. Liu, Z. Wang, Y. Li, *Mater. Horiz.* **2020**, *7*, 746 – 761.
[42] A. J. Surman, M. Rodriguez-Garcia, Y. M. Abul-Haija, G. J. T. Cooper, P. S. Gromski, R. Turk-MacLeod, M. Mullin, C. Mathis, S. I. Walker, L. Cronin, *Proc. Natl. Acad. Sci. USA* **2019**, *116*, 5387 – 5392.
[43] A. P. Jathoul, J. Laufer, O. Ogunlade, B. Treeby, B. Cox, E. Zhang, P. Johnson, A. R. Pizzey, B. Philip, T. Marafioti, M. F. Lythgoe, R. B. Pedley, M. A. Pule, P. Beard, *Nat. Photonics* **2015**, *9*, 239 – 246.

Manuscript received: December 16, 2020
Accepted manuscript online: January 11, 2021
Version of record online: February 24, 2021

